Heliyon

Received:
1 December 2018
Revised:
15 January 2019
Accepted:
16 January 2019

Cite as: Sk. Md. Arif, Aindrila Bera, Manas Ghosh. Tuning diamagnetic susceptibility of impurity doped quantum dots by noise-binding energy interplay.
Heliyon 5 (2019) e01147.
doi: 10.1016/j.heliyon.2019.e01147

Tuning diamagnetic susceptibility of impurity doped quantum dots by noise-binding energy interplay

Sk. Md. Arif, Aindrila Bera, Manas Ghosh *

Department of Chemistry, Physical Chemistry Section, Visva-Bharati University, Santiniketan, Birbhum 731235, West Bengal, India

* Corresponding author.
E-mail address: manasghosh.chem@visva-bharati.ac.in (M. Ghosh).

Abstract

In the present work we explore the role of *noise-binding energy (BE) interplay* on the *diamagnetic susceptibility (DMS)* of doped *GaAs* quantum dot (QD). *Gaussian white noise* has been invoked for the above exploration. And Gaussian impurity acts as a dopant in the present study. The mode of inclusion of noise to the system significantly affects the above interplay and thus prominently modulates the DMS profile. The outcomes of the inspection unfolds the way by which DMS of doped QD can be regulated by prudent adjustment of noise-BE interaction.

Keywords: Materials science

1. Introduction

Quantum wells (QWLs), quantum wires (QWRs) and quantum dots (QDs) are some mentionable examples of low-dimensional semiconductor systems (LDSS) that have collected serious recognition in the last few decades. There are two reasons that appear to underlie such widespread recognition. Firstly, the nanoscale dimension of LDSS results into profound enhancement of quantum effects in their physical properties (electrical, optical, magnetic etc.) in comparison with the bulk materials. Moreover, LDSS-based devices are also renowned for their high design-flexibility.

https://doi.org/10.1016/j.heliyon.2019.e01147

The enhanced quantum effects and the said flexibility have earmarked LDSS as potential ingredients for manufacturing several high-performance microelectronic and optoelectronic devices. Secondly, from a pedagogic viewpoint; cultivation of LDSS physics provides revisit of many fundamental quantum mechanical concepts [1]. Entry of impurity (dopant) to LDSS induces an interplay between the inherent confinement potential of LDSS and the dopant potential. Such interplay gives rise to an effective confinement potential that discernibly alters several physical properties of LDSS from that of an impurity-free state. These modified physical properties mark recognizable signature on the technology-related aspects of LDSS. Naturally, investigations on LDSS physics with impurity contamination have been performed in abundance over the last few decades [2, 3, 4, 5, 6, 7, 8, 9, 10, 11, 12, 13, 14, 15, 16, 17, 18, 19, 20, 21, 22].

Study of magnetic properties of LDSS assumes importance in order to understand electronic magnetism in nanoscale domain which often involves interesting physics [23, 24, 25, 26, 27, 28]. Such studies are done in presence of applied magnetic field which changes the energy spectrum of LDSS. A changed energy spectrum, in effect, regulates the performance of optoelectronic devices [29]. Furthermore, studies of magnetic properties of LDSS are also found to be relevant in several related fields. These fields include particle dynamics of LDSS in an external magnetic field (connected with spintronics), quantum electronic structure of LDSS [26], semiconductor-metal transitions in LDSS [30], and various other applications. Doping of impurity into LDSS further increases the intricacies in its magnetic properties [31, 32, 33, 34, 35].

Diamagnetic susceptibility (DMS) is an important magnetic property which has been extensively studied for LDSS doped with impurity. Study of DMS maintains close linkage with development of spintronics, quantum chaos, electronic conductivity and various other technological applications of electronic and optoelectronic devices [34, 35, 36, 37, 38, 39, 40, 41, 42, 43, 44, 45, 46]. Therefore, in view of comprehensive investigation on DMS of LDSS; often, contribution of various physical quantities e.g. effective mass [47, 48], dielectric constant [49, 50], hydrostatic pressure and temperature [51, 52, 53, 54, 55] has been explored in detail.

The output of LDSS-based devices is often influenced by the presence of *noise*. Incorporation of noise to the system can be done externally in different ways (also called ‘modes’ or ‘pathways’) leading to different consequences. Two such pathways are called *additive* and *multiplicative* based on their different extents of interaction with the system. The physical properties of system are also naturally perturbed by the presence of noise. And the size of change in the physical properties of the system noticeably depends on the mode of introduction of noise as mentioned above. It is therefore quite sensible to explore the noise effects on different physical properties of LDSS which ultimately governs the functioning of LDSS based devices.

 https://doi.org/10.1016/j.heliyon.2019.e01147

In this communication we inspect how DMS (χ_{dia}) of 2-d $GaAs$ QD depends on the *binding energy (BE)* of the system under the governance of noise. The harmonic oscillator potential defines the $x - y$ confinement whereas the z-confinement is provided by a perpendicular magnetic field. The QD contains *Gaussian* impurity as dopant and is simultaneously fed with *Gaussian white noise* either via additive or multiplicative route (modes). Variation of χ_{dia} against magnetic field strength (B) has been monitored for different values of BE of the system. And this monitoring is carried out both with and without noise. The study unveils how BE of the system influences its DMS with some additional delicacies offered by noise.

2. Methods

The Hamiltonian (H_0) describing the system can be given by

$$H_0 = H_0' + V_{imp} + V_{noise}. \tag{1}$$

H_0' is the dopant-free Hamiltonian. Considering harmonic confinement in the $x - y$ plane and vertical magnetic field, H_0', with the help of effective mass approximation, can be given by

$$H_0' = \frac{1}{2m^*}\left[-i\hbar\nabla + \frac{e}{c}\mathbf{A}\right]^2 + \frac{1}{2}m^*\omega_0^2(x^2 + y^2). \tag{2}$$

m^* and ω_0 denote the effective mass of the electron and the harmonic confinement frequency, respectively. The vector potential $\mathbf{A}$ has been chosen to be $A = (By, 0, 0)$, where B is the strength of the magnetic field. H_0' of eqn(2) can be transformed to

$$H_0' = -\frac{\hbar^2}{2m^*}\left(\frac{\partial^2}{\partial x^2} + \frac{\partial^2}{\partial y^2}\right) + \frac{1}{2}m^*\omega_0^2x^2 + \frac{1}{2}m^*\Omega^2y^2 - i\hbar\omega_c y\frac{\partial}{\partial x}. \tag{3}$$

In eqn(3) $\Omega(= \sqrt{\omega_0^2 + \omega_c^2})$ represents the effective confinement frequency in the y-direction and $\omega_c(= \frac{eB}{m^*c})$ stands for the cyclotron frequency. V_{imp} refers to the impurity (dopant) potential and reads $V_{imp} = V_0\ e^{-\gamma\left[(x-x_0)^2+(y-y_0)^2\right]}$. Here (x_0, y_0), V_0 and $\gamma^{-1/2}$ stand for the dopant site (coordinate), dopant potential strength, and the spatial domain where the impurity potential is effective, respectively. V_{noise} of eqn(1) stands for the noise part of the Hamiltonian. In the present work Gaussian white noise has been exploited having features like zero average and spatial δ-correlation. Introduction of noise to the system is carried out in two different routes (called additive and multiplicative) which actually guide the size of the system-noise interplay. The direct product basis of the harmonic oscillator eigenstates has been used to construct the Hamiltonian matrix (H_0). The energy levels and the eigenstates of the system are obtained by diagonalizing H_0 after performing the routine convergence test.

 https://doi.org/10.1016/j.heliyon.2019.e01147

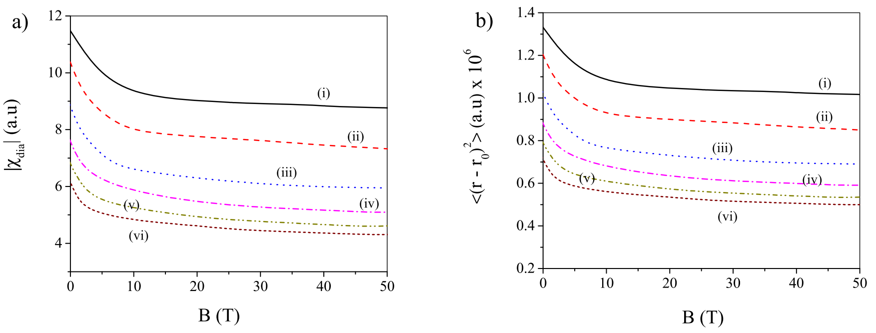

Figure 1. Plots of (a) $|\chi_{dia}|$ and (b) $\langle (r-r_0)^2 \rangle$ against B for six different values of BE without noise: (i) 0 meV, (ii) 50 meV, (iii) 125 meV, (iv) 150 meV, (v) 200 meV and (vi) 250 meV.

According to the Langevin formula DMS or Larmor DMS (in a.u.) is given by [44, 48]

$$\chi_{dia} = -\frac{e^2}{6m^*\varepsilon c^2}\langle (r-r_0)^2 \rangle, \tag{4}$$

where r_0 is the dopant coordinate. $\langle (r-r_0)^2 \rangle$ stands for the variance of the separation between the impurity and the dot confinement center.

The ground state binding energy (E_B) is given by

$$E_B = E_0 - E, \tag{5}$$

where E_0 and E are the ground state energies without and with impurity, respectively.

3. Results and discussion

In the present study we have used $\varepsilon = 12.4$ and $m^* = 0.067m_0$ (m_0 is the mass of electron in vacuum). Moreover, during the study a few relevant parameters assume following fixed values: $\hbar\omega_0 = 250.0$ meV, $V_0 = 280.0$ meV, $r_0 = 0.0$ nm and $\zeta = 1.0 \times 10^{-4}$, where ζ is the noise strength. χ_{dia} and BE have been calculated by using eqn(4) and eqn(5), respectively.

We begin with the plot of absolute value of DMS ($|\chi_{dia}|$) against magnetic field strength (B) without noise for six different values of BE (values are given in the figure caption) [Figure 1a].

DMS invariably displays steady drop as B increases [40, 41, 42, 44, 50]. However, at large B, DMS exhibits some sort of steady magnitude [50]. The said decrease in the magnitude of DMS originates from the drop in the mean square separation of impurity from the dot confinement center i.e. $\langle (r-r_0)^2 \rangle$. Aforesaid drop takes place because a steadily increasing B enforces enhanced geometrical confinement on the system thereby arresting the spread of the wave function in the vicinity of the

 https://doi.org/10.1016/j.heliyon.2019.e01147

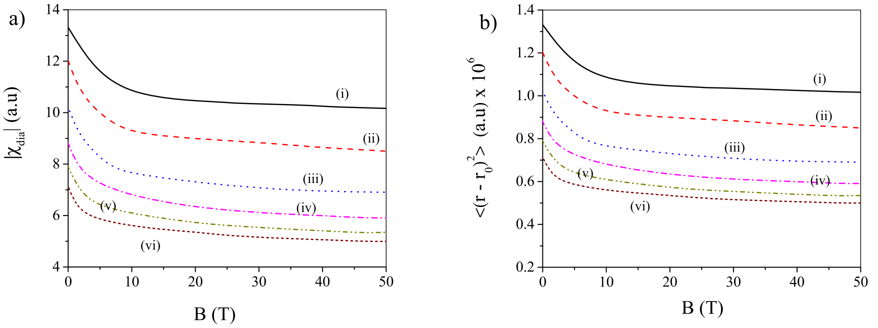

Figure 2. Plots of (a) $|\chi_{dia}|$ and (b) $\langle (r - r_0)^2 \rangle$ against $\boldsymbol{B}$ for six different values of BE when additive noise is present: (i) 0 meV, (ii) 50 meV, (iii) 125 meV, (iv) 150 meV, (v) 200 meV and (vi) 250 meV.

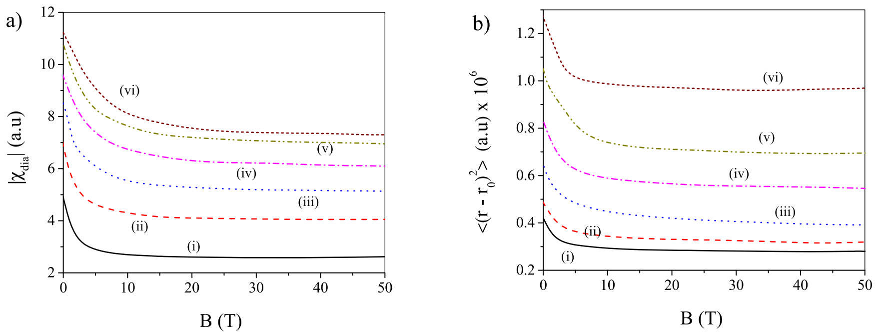

Figure 3. Plots of (a) $|\chi_{dia}|$ and (b) $\langle (r - r_0)^2 \rangle$ against $\boldsymbol{B}$ for six different values of BE when multiplicative noise is present: (i) 0 meV, (ii) 50 meV, (iii) 125 meV, (iv) 150 meV, (v) 200 meV and (vi) 250 meV.

impurity site [40, 50]. And the saturation which is visible at high $\boldsymbol{B}$ value reflects somewhat steady separation ($\sqrt{\langle (r - r_0)^2 \rangle}$) between electron and impurity [50]. Moreover, an increase in BE happens to cause a steady fall in the magnitude of DMS. Figure 1b plots the profiles of $\langle (r - r_0)^2 \rangle$ against $\boldsymbol{B}$ in absence of noise for identical values of BE as before and supports the earlier observation.

Figures 2a and 2b represent the plots of $|\chi_{dia}|$ vs $\boldsymbol{B}$ and $\langle (r - r_0)^2 \rangle$ vs $\boldsymbol{B}$, respectively, with additive noise, for same set of BE values. The plots do not reveal any noticeable qualitative change in their features from that under noise-free state; except a change in the magnitude of DMS. Hence, introduction of additive noise refrains from affecting the noise-free system sufficiently so far as DMS is concerned. Furthermore, the additive noise-BE interplay also does not alter the nature of variation of DMS with BE from that when noise effect becomes absent.

Noticeable change in the DMS profile becomes perceptible with the introduction of multiplicative noise. Figures 3a and 3b delineate the plots of $|\chi_{dia}|$ vs $\boldsymbol{B}$ and $\langle (r - r_0)^2 \rangle$ vs $\boldsymbol{B}$, respectively, with multiplicative noise, for same sequence of BE values. Just like previous two situations, here also the magnitude of DMS reveals regular fall with increase in $\boldsymbol{B}$ because of reduction in the magnitude of $\langle (r - r_0)^2 \rangle$. Thus, the gradually increasing spatial restriction on the electronic wave function

 https://doi.org/10.1016/j.heliyon.2019.e01147

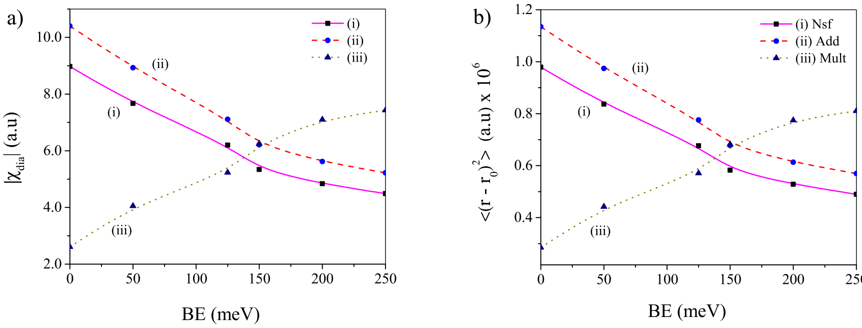

Figure 4. Plots of (a) $|\chi_{dia}|$ and (b) $\langle (r - r_0)^2 \rangle$ against BE at $B = 25$ T: (i) in absence of noise, (ii) while additive noise is operating and (iii) while multiplicative noise is operating.

that follows a regularly increasing magnetic field remains quite similar with and without noise; regardless of its mode. However, unlike previous two cases, here a monotonic increase in DMS magnitude is envisaged with increase in BE [Figure 3a]. The observation is also amply supported by mean square separation plot [Figure 3b]. Thus, the presence of multiplicative noise reverses the effect of noise-BE interplay on DMS magnitude from that of additive noise.

The effect of noise-BE interplay on DMS can be more clearly visualized with the plot of $|\chi_{dia}|$ against BE itself; under different sets of conditions and at a fixed value of $B = 25$ T [Figure 4a]. The plot exhibits persistent fall of DMS (magnitude) as BE increases both without noise [Figure 4a(i)] and when additive noise is present [Figure 4a(ii)]. Corresponding mean square separation plot also corroborates the above findings [Figure 4b(i–ii)]. The observation clearly indicates progressively increasing spatial constraint on wave function that accompanies a rise in BE of the system under above two conditions. However, applied multiplicative noise completely reverses the scenario as now we observe a persistent growth in the DMS magnitude with increase in BE [Figure 4a(iii)]. Thus, multiplicative noise causes steadfast enhancement of the spatial stretch of wave function as BE increases. The relevant mean square distance plot also runs in agreement with the above outcome [Figure 4b(iii)]. The nature of noise-BE interaction thus prominently anchors on the mode of application (additive/multiplicative) of noise, and, in consequence, alters the DMS profile in contrasting ways. In the present context, it is basically the way noise couples with the system coordinates that matters most. Multiplicative noise induces more intensive coupling with the system coordinates than its additive neighbor. Thus, the noise-BE interaction becomes also different for these two different pathways giving rise to contrasting features in the observed DMS profile.

 https://doi.org/10.1016/j.heliyon.2019.e01147

4. Conclusion

DMS of doped *GaAs* QD has been found to be discernibly dependent on the noise-binding energy interplay. An increase in the magnetic field strength invariably reduces the magnitude of DMS; regardless of presence of noise. Both under noise-free condition and in presence of additive noise DMS declines as BE increases. However, a shift from additive to multiplicative mode of applying noise changes the scenario whence DMS displays clear enhancement with increase in BE. The findings show prolific means of regulating the DMS of doped QD system by appropriate control of noise-BE interaction.

Declarations

Author contribution statement

Sk. Md. Arif, Aindrila Bera, Manas Ghosh: Conceived and designed the experiments; Performed the experiments; Analyzed and interpreted the data; Contributed reagents, materials, analysis tools or data; Wrote the paper.

Funding statement

This research did not receive any specific grant from funding agencies in the public, commercial, or not-for-profit sectors.

Competing interest statement

The authors declare no conflict of interest.

Additional information

No additional information is available for this paper.

Acknowledgements

The authors S. M. A., A. B. and M. G. thank D. S. T-F. I. S. T (Govt. of India) and U. G. C.- S. A. P (Govt. of India) for support. Special thanks to Mrs. Anuja Ghosh for her sincere cooperation.

https://doi.org/10.1016/j.heliyon.2019.e01147

References

[1] B. Boyacioglu, A. Chatterjee, Dia- and paramagnetism and total susceptibility of *GaAs* quantum dots with Gaussian confinement, Physica E 44 (2012) 1826–1831.

[2] İ. Karabulut, H. Şafak, M. Tomak, Nonlinear optical rectification in asymmetrical semiparabolic quantum wells, Solid State Commun. 135 (2005) 735–738.

[3] İ. Karabulut, Ü. Atav, H. Şafak, M. Tomak, Linear and nonlinear intersubband optical absorptions in an asymmetric rectangular quantum well, Eur. Phys. J. B 55 (2007) 283–288.

[4] A. Özmen, Y. Yakar, B. Çakir, Ü. Atav, Computation of the oscillator strength and absorption coefficients for the intersubband transitions of the spherical quantum dot, Opt. Commun. 282 (2009) 3999–4004.

[5] B. Chen, K.-X. Guo, Z.-L. Liu, R.-Z. Wang, Y.-B. Zheng, B. Li, Second-order nonlinear optical susceptibilities in asymmetric coupled quantum wells, J. Phys. Condens. Matter 20 (2008) 255214.

[6] S. Şakiroğlu, F. Ungan, U. Yesilgul, M.E. Mora-Ramos, C.A. Duque, E. Kasapoglu, H. Sari, I. Sökmen, Nonlinear optical rectification and the second and third harmonic generation in Pöschl–Teller quantum well under the intense laser field, Phys. Lett. A 376 (2012) 1875–1880.

[7] F. Ungan, J.C. Mertínez-Orozco, R.L. Restrepo, M.E. Mora-Ramos, E. Kasapoglu, C.A. Duque, Nonlinear optical rectification and second-harmonic generation in a semi-parabolic quantum well under intense laser field: effects of electric and magnetic fields, Superlattices Microstruct. 81 (2015) 26–33.

[8] H. Hassanabadi, G. Liu, L. Lu, Nonlinear optical rectification and the second-harmonic generation in semi-parabolic and semi-inverse quantum wells, Solid State Commun. 152 (2012) 1761–1766.

[9] S. Baskoutas, E. Paspalakis, A.F. Terzis, Effects of excitons in nonlinear optical rectification in semiparabolic quantum dots, Phys. Rev. B 74 (2006) 153306.

[10] S. Baskoutas, E. Paspalakis, A.F. Terzis, Electronic structure and nonlinear optical rectification in a quantum dot: effects of impurities and external electric field, J. Phys. Condens. Matter 19 (2007) 395024.

[11] G. Liu, K.-X. Guo, H. Hassanabadi, L. Lu, Linear and nonlinear optical properties in a disk-shaped quantum dot with a parabolic potential plus

 https://doi.org/10.1016/j.heliyon.2019.e01147

a hyperbolic potential in a static magnetic field, Physica B 407 (2012) 3676–3682.

[12] B. Çakir, Y. Yakar, A. Özmen, M. Özgür Sezer, M. Şahin, Linear and nonlinear optical absorption coefficients and binding energy of a spherical quantum dot, Superlattices Microstruct. 47 (2010) 556–566.

[13] Z. Zeng, C.S. Garoufalis, A.F. Terzis, S. Baskoutas, Linear and nonlinear optical properties of ZnS/ZnO core shell quantum dots: effect of shell thickness, impurity, and dielectric environment, J. Appl. Phys. 114 (2013) 023510.

[14] M. Kirak, S. Yilmaz, M. Şahin, M. Gençasian, The electric field effects on the binding energies and the nonlinear optical properties of a donor impurity in a spherical quantum dot, J. Appl. Phys. 109 (2011) 094309.

[15] C.A. Duque, N. Porras-Montenegro, Z. Barticevic, M. Pacheco, L.E. Oliveira, Effects of applied magnetic fields and hydrostatic pressure on the optical transitions in self-assembled $InAs/GaAs$ quantum dots, J. Phys. Condens. Matter 18 (2006) 1877.

[16] M. Pacheco, Z. Barticevic, Optical response of a quantum dot superlattice under electric and magnetic fields, Phys. Rev. B 64 (2001) 033406.

[17] M.G. Barseghyan, C.A. Duque, E.C. Niculescu, A. Radu, Intense laser field effects on the linear and nonlinear optical properties in a semiconductor quantum wire with triangle cross section, Superlattices Microstruct. 66 (2014) 10–22.

[18] H.M. Baghramyan, M.G. Barseghyan, A.A. Kirakosyan, R.L. Restrepo, C.A. Duque, Linear and nonlinear optical absorption coefficients in $GaAs/Ga_{1-x}Al_xAs$ concentric double quantum rings: effects of hydrostatic pressure and aluminium concentration, J. Lumin. 134 (2013) 594–599.

[19] A. Hakimyfard, M.G. Barseghyan, A.A. Kirakosyan, Simultaneous effects of pressure and magnetic field on intersubband optical transitions in Pöschl–Teller quantum well, Physica E 41 (2009) 1596–1599.

[20] W. Xie, Nonlinear optical properties of a hydrogenic donor quantum dot, Phys. Lett. A 372 (2008) 5498–5500.

[21] W. Xie, Impurity effects on optical property of a spherical quantum dot in the presence of an electric field, Physica B 405 (2010) 3436–3440.

[22] S. Liang, W. Xie, Effects of the hydrostatic pressure and temperature on optical properties of a hydrogenic impurity in the disc-shaped quantum dot, Physica B 406 (2011) 2224–2230.

 https://doi.org/10.1016/j.heliyon.2019.e01147
2405-8440/

[23] O. Voskoboynikov, O. Bauga, C.P. Lee, O. Tretyak, Magnetic properties of parabolic quantum dots in the presence of the spin-orbit interaction, J. Appl. Phys. 94 (2003) 5891–5895.

[24] O. Voskoboynikov, C.P. Lee, Magnetization and magnetic susceptibility of $InAs$ nano-rings, Physica E 20 (2004) 278–281.

[25] Y. Li, Magnetization and Magnetic susceptibility in nanaoscale vertically coupled semiconductor quantum rings, J. Comput. Electron. 4 (2005) 135–138.

[26] J.J. Climente, J. Planelles, J.L. Movilla, Magnetization of nanoscopic quantum rings and dots, Phys. Rev. B 70 (2004) 081301(R) (4 pages).

[27] Y.P. Krasny, N.P. Kovalenko, U. Krey, L. Jacak, Paramagnetic-diamagnetic interplay in quantum dots for non-zero temperatures, J. Phys. Condens. Matter 13 (2001) 4341–4358.

[28] R. Khordad, Simultaneous effects of electron-electron interactions, Rashba spin-orbit interaction and magnetic field on susceptibility of quantum dots, J. Magn. Magn. Mater. 449 (2018) 510–514.

[29] E.C. Niculescu, C. Stan, M. Cristea, C. Truscă, Magnetic-field dependence of the impurity states in a dome-shaped quantum dot, Chem. Phys. 493 (2017) 32–41.

[30] A.J. Peter, K. Navaneethakrishnan, Semiconductor-metal transition in a quasi two-dimensional system, Solid State Commun. 120 (2001) 393–396.

[31] A. Boda, A. Chatterjee, Transition energies and magnetic properties of a neutral donor complex in a Gaussian $GaAs$ quantum dot, Superlattices Microstruct. 97 (2016) 268–276.

[32] S. Elagoz, R. Amca, S. Kutlu, I. Sökmen, Shallow impurity binding energy in lateral parabolic confinement under an external magnetic field, Superlattices Microstruct. 44 (2008) 802–808.

[33] S. Elagoz, P. Başer, U. Yahşib, The magnetic field dependency of hydrogenic impurity binding energy under inverse lateral parabolic potential, Physica B 403 (2008) 3879–3882.

[34] P. Nithiananthi, K. Jayakumar, Diamagnetic susceptibility of hydrogenic donor impurity in low-dimensional semiconducting systems, Solid State Commun. 137 (2006) 427–430.

[35] P. Nithiananthi, K. Jayakumar, Diamagnetic susceptibility of hydrogenic donor impurity in low lying excited states in a quantum well, Superlattices Microstruct. 40 (2006) 174–179.

 https://doi.org/10.1016/j.heliyon.2019.e01147

[36] N.M. Irulayee, K. Navaneethakrishnan, Diamagnetic susceptibility of a shallow donor in a quantum well, Physica E 41 (2008) 193–195.

[37] A.M.J.D. Reuben, K. Jayakumar, Diamagnetic susceptibility of a hydrogenic donor in a quantum dot, Phys. Status Solidi B 243 (2006) 4020–4024.

[38] R. Khordad, Diamagnetic susceptibility of a hydrogenic donor impurity in a V-groove $GaAs/Ga_{1-x}Al_xAs$ quantum wire, Eur. Phys. J. B 78 (2010) 399–403.

[39] K. Rahmani, I. Zorkani, A. Jorio, Diamagnetic susceptibility of a confined donor in inhomogeneous quantum dots, Phys. Scr. 83 (2011) 035701.

[40] J.J. Sharkey, C. Yoo, A.J. Peter, Magnetic field induced diamagnetic susceptibility of a hydrogenic donor in a $GaN/AlGaN$ quantum dot, Superlattices Microstruct. 48 (2010) 248–255.

[41] M. Köksal, E. Kilicarslan, H. Sari, I. Sökmen, Magnetic-field effect on the diamagnetic susceptibility of hydrogenic impurities in quantum well-wires, Physica B 404 (2009) 3850–3854.

[42] E. Kilicarslan, S. Sakiroğlu, E. Kasapoğlu, H. Sari, I. Sökmen, The effect of nitrogen on the diamagnetic susceptibility of a donor in $Ga_xIn_{1-x}N_yAs_{1-y}/GaAs$ quantum well under the magnetic field, Superlattices Microstruct. 48 (2010) 305–311.

[43] A. Boda, A. Chatterjee, Effect of an external magnetic field on the binding energy, magnetic moment and susceptibility of an off-center donor complex in a Gaussian quantum dot, Physica B 448 (2014) 244–246.

[44] A. Mmadi, K. Rahmani, I. Zorkani, A. Jorio, Diamagnetic susceptibility of a magneto-donor in inhomogeneous quantum dots, Superlattices Microstruct. 57 (2013) 27–36.

[45] G. Rezaei, N.A. Doostimotlagh, B. Vaseghi, Conduction band non-parabolicity effect on the binding energy and diamagnetic susceptibility of an on-center hydrogenic impurity in spherical quantum dots, Physica E 43 (2011) 1087–1090.

[46] Gh. Safarpour, M. Barati, M. Moradi, S. Davatolhagh, A. Zamani, Binding energy and diamagnetic susceptibility of an on-center hydrogenic donor impurity in a spherical quantum dot placed at the center of a cylindrical nanowire, Superlattices Microstruct. 52 (2012) 387–397.

[47] S. Rajashabala, K. Navaneethakrishnan, Effects of dielectric screening and position dependent effective mass on donor binding energies and on

diamagnetic susceptibility in a quantum well, Superlattices Microstruct. 43 (2008) 247–261.

[48] E. Kasapoğlu, F. Ungan, H. Sari, I. Sökmen, The diamagnetic susceptibilities of donors in quantum wells with anisotropic effective mass, Superlattices Microstruct. 46 (2009) 817–822.

[49] M. Latha, S. Rajashabala, K. Navaneethakrishnan, Effect of dielectric screening on the binding energies and diamagnetic susceptibility of a donor in a quantum well wire, Phys. Status Solidi B 243 (2006) 1219–1228.

[50] E. Kilicarslan, S. Sakiroğlu, M. Köksal, H. Sari, I. Sökmen, The effects of the magnetic field and dielectric screening on the diamagnetic susceptibility of a donor in a quantum well with anisotropic effective mass, Physica E 42 (2010) 1531–1535.

[51] G. Rezaei, N.A. Doostimotlagh, External electric field, hydrostatic pressure and conduction band non-parabolicity effects on the binding energy and the diamagnetic susceptibility of hydrogenic impurity quantum dot, Physica E 44 (2012) 833–838.

[52] B. Vaseghi, T. Sajadi, Simultaneous effects of pressure and temperature on the binding energy and diamagnetic susceptibility of a laser dressed donor in a spherical quantum dot, Physica B 407 (2012) 2790–2793.

[53] Gh. Safarpour, A. Jamasb, M. Dialameh, S. Yazdanpanahi, The effect of hydrostatic pressure on the binding energy and diamagnetic susceptibility of a laser dressed donor impurity in a $GaAs/GaAlAs$ nanowire superlattice, Superlattices Microstruct. 76 (2014) 442–452.

[54] G. Rezaei, N.A. Doostimotlagh, B. Vaseghi Commun, Simultaneous effects of hydrostatic pressure and conduction band non-parabolicity on binding energies and diamagnetic susceptibility of a hydrogenic impurity in spherical quantum dots, Commun. Theor. Phys. 56 (2011) 377–381.

[55] R. Khordad, N. Fathizadeh, Simultaneous effects of temperature and pressure on diamagnetic susceptibility of a shallow donor in a quantum antidot, Physica B 407 (2012) 1301–1305.